

Mixed Neural Network Approach for Temporal Sleep Stage Classification

Hao Dong, Akara Supratak, Wei Pan, Chao Wu, Paul M. Matthews and Yike Guo*

Abstract—This paper proposes a practical approach to addressing limitations posed by use of single active electrodes in applications for sleep stage classification. Electroencephalography (EEG)-based characterizations of sleep stage progression contribute the diagnosis and monitoring of the many pathologies of sleep. Several prior reports have explored ways of automating the analysis of sleep EEG and of reducing the complexity of the data needed for reliable discrimination of sleep stages in order to make it possible to perform sleep studies at lower cost in the home (rather than only in specialized clinical facilities). However, these reports have involved recordings from electrodes placed on the cranial vertex or occiput, which can be uncomfortable or difficult for subjects to position. Those that have utilized single EEG channels which contain less sleep information, have showed poor classification performance. We have taken advantage of Rectifier Neural Network for feature detection and Long Short-Term Memory (LSTM) network for sequential data learning to optimize classification performance with single electrode recordings. After exploring alternative electrode placements, we found a comfortable configuration of a single-channel EEG on the forehead and have shown that it can be integrated with additional electrodes for simultaneous recording of the electrooculogram (EOG). Evaluation of data from 62 people (with 494 hours sleep) demonstrated better performance of our analytical algorithm for automated sleep classification than existing approaches using vertex or occipital electrode placements. Use of this recording configuration with neural network deconvolution promises to make clinically indicated home sleep studies practical.

Index Terms—Sleep Stage Classification, Electroencephalography, EEG, Deep Learning, Long Short-Term Memory

I. INTRODUCTION

People spend approximately one-third of their life sleeping. Sleep related disorders, such as sleep apnea, insomnia, narcolepsy, severely affect the quality of life for a large amount of proportion of the population. For example, about 33% of general population reports suffering from insomnia [1]. For accurate diagnosis of sleep disorders, all-night polysomnographic (PSG) recording including an electroencephalogram (EEG), electrooculogram (EOG) and electromyogram (EMG), followed by expert manual scoring of sleep stages and their

progression according to standard guidelines is needed [2], [3]. High costs and limited availability of specialized facilities limits their use.

As home sleep monitoring and automatic sleep stage scoring could reduce costs and increase access to diagnostic sleep studies, there has been interest in coupling the development of simple, wearable EEG recording devices with automated sleep stage classifications. Three main challenges to the automatic sleep stage classification have been identified:

Challenge 1. Heterogeneity People have different cranial structures and vary demographically and physiologically in ways that influence EEG patterns in sleep. For example, about 10% people do not generate alpha rhythm during stage W, and a further 10% generate only limited alpha rhythm [3]. For these subjects, American Association of Sleep Medicine (AASM) guidelines suggest use of alternative criteria for classification of stages W and N1.

Challenge 2. Temporal Pattern Recognition Scoring sleep stage is a sequential problem [3], as sleep stage scoring depends not only on temporally local features but also on prior epochs time. For example, the onset of stage N2 depends on whether K complex or sleep spindles occurs early or the last half of the previous epoch [3]; stage N2 can be classified even without K complexes or sleep spindles. Rapid eye movement sleep (REM) classification also depends on the features from prior EEG epochs, e.g., an epoch can be scored as REM, even in the absence of rapid eye movements, if the chin EMG tone is low and at low amplitude and there is mixed frequency EEG activity without K complexes or sleep spindles.

Challenge 3. Comfort Previous reports [4], [5], [6], [7] described home sleep EEG recording with montages including central, occipital and parietal electrode ¹, which better detect sleep spindles, vertex sharp waves and alpha rhythm than do frontal electrode (Table I). However, these EEG positions demand placement of the electrodes in hairy regions of scalp, demanding careful placement and adhesive paste to minimize movement related noise, and can lead to limitation of head movement and discomfort during sleep [10].

A recent study [4] evaluated accuracy of classification with Fpz-Cz channel [8], using a Complex Morlet wavelets transform for feature extraction and Stacked Sparse Autoencoders for classification. This showed that including the features from neighboring epochs can improve the classification performance. It also highlighted a bias towards misclassification

Hao Dong is with Data Science Institute, Imperial College London, UK, SW7 2AZ e-mail: hao.dong11@imperial.ac.uk

Akara Supratak is with Data Science Institute, Imperial College London, UK, SW7 2AZ e-mail: akara.supratak12@imperial.ac.uk

Wei Pan is with Data Science Institute, Imperial College London, UK, SW7 2AZ e-mail: w.pan11@imperial.ac.uk

Chao Wu is with Data Science Institute, Imperial College London, UK, SW7 2AZ e-mail: chao.wu@imperial.ac.uk

Paul M. Matthews is with Division of Brain Sciences in the Department of Medicine, Imperial College London, UK, SW7 2AZ e-mail: p.matthews@imperial.ac.uk

Yike Guo is with Data Science Institute, Imperial College London, UK, SW7 2AZ e-mail: y.guo@imperial.ac.uk. *corresponding author

¹The location of scalp electrodes for sleep scoring is shown in Fig. 1, following the international 10/20 system, in which each site has a letter to identify the lobe and a number to identify the hemisphere location.

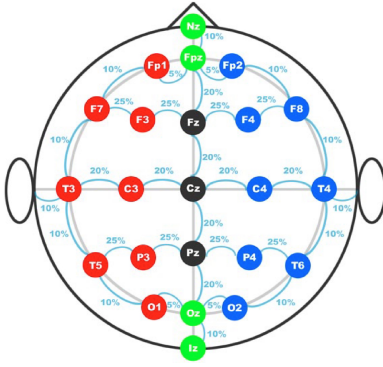


Fig. 1. The international 10/20 EEG system [26]. The letters F, T, C, P and O refer to frontal, temporal, central, parietal and occipital lobes placements, respectively. The even numbers refer to electrode positions on the right hemisphere, the odd numbers refer to electrode positions on the left hemisphere and the 'z' refers to electrode placement on the mid line of the head. Additionally, A1 and A2 define position on the left and right earlobes, respectively.

of epochs as the overall most frequently occurring class (stage N2) because of the inherent imbalance in occurrence of the different sleep stages. To solve the imbalance problem, the author used a down-sampling method to generate new, balanced dataset in which every sleep stage is equally represented. To use more information from the original training dataset, the authors generated new "balanced" datasets and trained individual networks using data from each of their subjects (ensemble learning). However, to obtain one prediction, feed-forward propagations on each of the individual networks are required. This is inefficient, although it improves accuracy. Here, we have chosen an alternative "ensemble learning" method that gains in efficiency by using dropout [19].

Other reports describe ways in which classification accuracy can be improved by supplementing data with EEG recordings from central, occipital or parietal electrode. For example, [5] evaluated a method by using a C3-A1 channel. In [6], alternative approaches using a C3-A2 and the Pz-Oz channels were described. The author used multi-scale entropy (MSE) and autoregressive (AR) models as features, and then trained a linear discriminant analysis (LDA) model as a classifier. In [7], classification was based on the Cz-Pz channel. However, all these three studies evaluated their methods without any type of cross-validation and one [5] trained the classifier using signals from all subjects, which meant that training and testing data were not independent.

In our approach, we propose use of a Mixed Neural Network (MNN) to solve both the population heterogeneity and temporal pattern recognition problems. Our MNN is composed of a Rectifier Neural Network which suitable for detecting naturally sparse patterns [17], and a Long Short-Term Memory (LSTM) for detection of temporally sequential patterns [23]. We will describe the details in Section II-C. For signal recording, we propose a novel configuration that combines low frontal electrode for EEG signal detection with another electrode for electrooculography (EOG). During periods without eye movement, the latter electrodes act as reference electrodes (analogous to A1 and A2). Through the full course of the

study, the EOG provides additional information for sleep scoring by detecting eye movements [11], [12].

TABLE II
PERFORMANCE OF LITERATURE

Method	F1					MF1	ACC
	W	N1	N2	N3	REM		
Fpz-Cz [4]	71.58	47.04	84.60	84.03	81.40	73.73	78.94
Cz-Pz [5]	91.45	47.62	82.59	74.21	77.81	74.74	82.57
C3-A2/Pz-Oz [6]	93.62	15.29	78.25	71.45	81.96	68.11	83.60
Cz-Pz [7]	85.95	20.86	84.78	84.28	85.95	72.36	82.93

II. METHODOLOGY

A. Sleep stage standards

There are two standards commonly used to define sleep stages: the Rechtschaffen and Kales (R&K) [2], and that developed by the American Academy of Sleep Medicine (AASM) [3]. The AASM standard adopted for this paper, classifies sleep into 5 different stages with one awake stage (W), three sleep stages (N1, N2, N3) corresponding to different depths of sleep, and one rapid eye movement stage (REM). Table I summarizes the waves and events of EEG during sleep included in the AASM standards. Each sleep staging decision is based on a 30 (or 20) seconds window of the physiological signals called an EEG epoch.

B. Features selection based on sleep physiology

The physiological features of sleep EEG can be typically characterized either in the time or frequency-domain (Table I).

1) *Spectral power of frequency bands*: Our approach uses time-frequency analysis to extract feature from each EEG epoch (Table III). We have chosen to use a conventional Fourier transform over other methods (e.g., complex Morlet wavelets) to allow us to strictly follow the AASM standards and then take advantage of neural network to further extract feature.

A short-time Fourier transform (STFT) [15] is used to extract temporal features. STFT extracts the frequency and phase content of a signal as it changes over time to generate a spectrogram. STFT has three parameters: the sliding window size, the overlap percentage, and the window function. The sliding window size defines the time interval of an EEG segment and controls the trade-off between frequency and temporal precision. e.g., increasing the window size will increase frequency precision, but decrease temporal precision. We allow segments to overlap to reduce artifacts at the boundaries of adjacent windows. Increasing the degree of overlap will decrease artifacts, but will also lead to higher computation costs. Window function is used to reduce the spectral leakage at the boundary of a sliding window.

In our experiment, the STFT was used to divide the 30 seconds EEG epochs into shorter segments of 5 seconds with serial overlaps of 70%. Each of the short EEG segments was windowed by hamming window function. After generating a

spectrogram by using STFT, the spectral power of different sub-bands were calculated by summing up the amplitude values in each segment to define the power spectrum density (PSD) [15]. The PSD is described below as (1), where x is the windowed raw EEG segment, $F(x)$ is the amplitude values after Fourier transform from the EEG segments and f_{min} and f_{max} are the minimum and maximum frequencies of given in Table III.

$$PSD = \sum_{i=f_{min}}^{f_{max}} F(x)_i \quad (1)$$

A 5-second sliding window can not always cover the whole period of the low-frequency slow eye movements [12], so they can be difficult to detect it using STFT even with zeropadding. To address this issue, the PSD of slow eye movement was captured by applying Fourier transform over the entire EEG epoch.

2) *Statistics of spectral power*: Additional information can be extracted from the spectral power. Some features such as alpha rhythm and sleep spindle usually appear regularly. The duration of each sub-band was estimated by averaging PSDs over an EEG epoch. Larger averaged PSD is equivalent to better continuation.

Low averaged and median PSD values with a high maximum PSD value appears as an occasional feature, such as K complexes and vertex shape waves. Moreover, the standard derivation of each sub-band evaluated the frequency fluctuation.

3) *Time domain*: The EEG amplitude is usually lower than $100\mu V$, while the EMG, EOG and movement artifact amplitudes are often higher. The maximum and minimum amplitudes of the raw EEG signal reflect artifact information. As the Shannon entropy of raw EEG signal [16] is sensitive to the amplitude distribution, it can additionally be used to derive related features from signal synchronization or amplitude.

C. Mixed neural network

The temporal physiological features as introduced in the previous section can serve as the input data which can feed into different classes of classification algorithms, e.g., logistic regression, supporting vector machine, etc. Unfortunately, the classification performance of these has been poor because they do not address the *temporal pattern recognition* challenge. Some of the physiological features are strongly correlated, although they may be incomplete relative to currently accepted sleep physiological descriptions. Further exploration in the feature space is needed. As emphasized earlier, any given sleep stage depends not only on the features at the moment, but also on those that are highly correlated in the past. Such temporal dependency needs to be considered.

Motivated by these considerations, two classes of deep neural networks are introduced: multi-layer perception (MLP) and a recurrent neural network (RNN) to address completeness and temporal correlations, respectively. As illustrated in Fig. 2, after independent applications, MLP and RNN are concatenated in our model.

In the end, a softmax function is introduced for classification. In summary, the key idea is to use a mixture of neural networks to "learn" new features for classification. This type of mixture is termed as *mixed neural network (MNN)*.

In Fig. 2, MNN specifies a modular structure for MLP, RNN and softmax respectively. For the MLP module, there are many latent parameters needed to be selected and tuned, such as the number of layers, number of units in each layer and the selection of nonlinear activation functions. Similar problem arises in RNN module as well, moreover, the structure of RNN needs to be specified *a priori*.

In our study, we choose a Rectifier Neural Network as the candidate for MLP module and Long-Short Term Memory architecture for RNN module. These selections are mainly based on an *ad-hoc* tests across various combinations of these parameters, especially the number of layers and number of units across layers. Nevertheless, we provide an analysis on the selection of rectifier function as the candidate nonlinear activation function in MLP module.

1) *Rectifier Neural Network*: A Rectifier Neural Network was used in the MLP module, where the function is described as follows:

$$f(x) = \max(0, x). \quad (2)$$

The rectifier network has proved to be able to optimize performance without any unsupervised pre-training on unlabelled data. It is well known that rectifying neurons performed better when the data is sparse compared to sigmoid and hyperbolic tangent neurons [17]. In our case, the EEG spectrum is a typical type of sparse data. First of all, only a few frequency bands will exist in any particular sleep stage. Secondly, the frequency activities are discontinuous, e.g., the alpha activity may only appear for about 50% of the epoch in stage W. Thirdly, different people may show different frequency amplitudes in same sleep stage. The rectifier is partially inspired by biological models, e.g., the percentage of neurons active at any time may be as low as 1 to 4% in human brain [18]; the Rectifier Neural Network is able to describe such sparse representations easily. For example, around 50% of the hidden units will output zeros, if the weights are uniformly initialized. With this characteristic, the rectifier neurons can automatically 'select' features, then the input selects a subset of active neurons.

In addition, the output is a linear function of the inputs, so the gradients from next RNN module are able to back-propagate well to all layers. This alleviate the "vanishing gradient" problem. As the spectrogram is used as input, the output of a rectifier neuron in the first hidden layer is the combination of PSDs features. Combinations of absent frequency bands output as zero with a rectifier, so their values will not effect the inputs of next layer. For discontinuous features and variation problem, the rectifier can represent whether these features exist by active or not.

Dropout is a popular technique for addressing overfitting in deep neural networks [19], [20]. This randomly sets input values and activation values to zero during training, resembling randomly disconnecting the neural units from one layer to the next. The dropout method is able to train a large number of

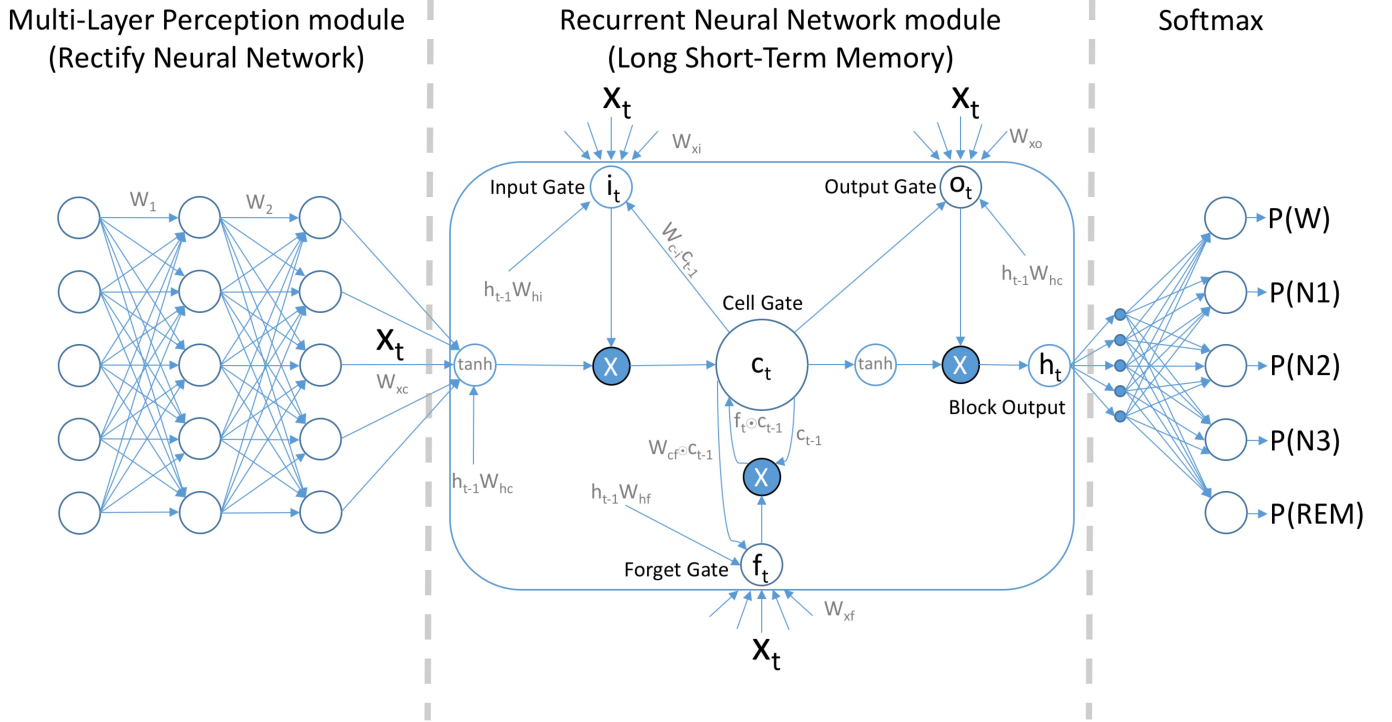


Fig. 2. Structure of mixed neural network; Rectify Neural Network was chosen as Multi-Layer Perception module; Long Short-Term Memory was chosen as Recurrent Neural Network module

different networks while allowing all of the networks to share the same weights for the hidden neuron. It can be considered as another form of ensemble learning [19], and has similarities to autoencoders that we have described previously [4].

In our work here, we set the dropout probability from input layer to first rectifier layer, from first rectifier layer to second rectifier layer, and from second rectifier layer to RNN module as 20%, 50% and 50%, respectively. We found empirically that this combination of dropout probabilities achieved the best performance, which is similar to the dropout experimental study on MNIST dataset [19].

Without the Rectifier Neural Network, the accuracy dropped by 3%. Moreover, in our experiment, we found the rectify activation function work better than sigmoid and hyperbolic tangent functions. It is also possible that this is caused by the non-linearities, e.g., when using sigmoid or hyperbolic tangent functions, even the input values are very high, the output will not change too much, because the output is close to 1.

2) *Long short-term memory*: Long short-term memory (LSTM) architecture is selected as the candidate in the RNN module. LSTM is well known to be capable of learning long-term dependencies problem [21], [23]. The advantage of LSTM is that it not only applied the current information to perform the present task, but also explicitly takes account to long-term information in the past which is a limitation of classic RNN architecture (the long-term dependency problem). Overall, the long term information memory is a key property of the LSTM architecture.

An illustrative example of long-term dependency problem

in sleep stages classification arises when a long period of N2 sleep shifts to stage N1 for several EEG epochs. If sleep spindles appear, the probability of reverting to stage N2 is higher than the probability of progressing to stage N3.

LSTM works better than classic RNN to handle the long gap between the relevant information. In [22], it is shown that the RNNs are unable to relationships with long-term information.

In this study, LSTM is implemented by the following formulas, which is the vanilla architecture. It should be noted that the vanilla LSTM outperformed than any other variations as shown in [24]. The function σ_h and σ_c are the hyperbolic tangent activation function applied to the block output and cell gate, the other σ functions are logistic sigmoid function. The element-wise multiplication (Hadamard product) of two vectors is denoted by \odot .

$$\begin{aligned}
 i_t &= \sigma_i(x_t W_{xi} + h_{t-1} W_{hi} + w_{ci} \odot c_{t-1} + b_i) && \text{input gate} \\
 f_t &= \sigma_f(x_t W_{xf} + h_{t-1} W_{hf} + w_{cf} \odot c_{t-1} + b_f) && \text{forget gate} \\
 c_t &= f_t \odot c_{t-1} + i_t \odot \sigma_c(x_t W_{xc} + h_{t-1} W_{hc} + b_c) && \text{cell state} \\
 o_t &= \sigma_o(x_t W_{xo} + h_{t-1} W_{ho} + w_{co} \odot c_t + b_o) && \text{output gate} \\
 h_t &= o_t \odot \sigma_h(c_t) && \text{block output}
 \end{aligned}$$

The key components of LSTM are the cell and forget gates, which are used to store information from previous inputs; note that all of the formulae above except those for the output gate are related as c_{t-1} , which stores prior state information. The forget gate f_t determines whether to 'forget' or 'remember' the current stage by putting a feedback on cell state.

3) *Output module*: After LSTM, multinomial classification (softmax regression) was applied as the output layer, which is widely used in various probabilistic multi-class classification problem. The softmax regression is the generalization of logistic regression to multiple categories, which is to predict the probability of inputs (x) belonging to each class (y). The number of output of softmax layer equal to the number of classes; as there are 5 stages in our classification, the number of output is 5.

D. Training the network

The MNN was trained by using stochastic gradient descent (SGD) [25] with a batch size of 500 examples and learning rate of 0.01 with momentum of 0.9. According to the softmax output and dropout of rectifier neural network, cross-entropy was used as the loss function without any kinds of weight decay.

E. Experimental Design

A open access dataset [9] was used to evaluate the proposed method. It includes data from 62 healthy subjects, aged from 23 to 73 years (29 men, 33 women). All recordings are from different subjects. The EEG epoch duration of each recording was 30 seconds and recordings were scored by a single sleep expert following the AASM standard. Sleep stages are labeled as stage W, N1, N2, N3, REM or unknown. The unknown stage only exists at the start and the end of recordings when the subjects were preparing to sleep or when the subjects are completing the recording. To evaluate the proposed method, only the in-bed part of the recording was taken, so the unknown stage was ignored.

The recording contains 20 EEG, 2 EOG, 1 ECG and 3 EMG channels, and all EEG channels are referential. This means that we are testing whether our method, which uses limited physiological data, approaches similar performance to the expert reader with a full set of bio-signal data. We used the derivation between F4 and EOG Left Horizon. They are placed near the hairline and outer-down canthus of left eye, none of which are placed on the skin with hair. This is the fundamental distinction of our method from prior studies, the motivation for which being demonstration of a proof of principle for a convenient and comfortable to home-based EEG recording electrode configuration.

To evaluate the Mixed Neural Network, we tried several models for the Rectifier Neural Network by varying the number of hidden layers (2 to 5), the number of hidden units in rectifying layer (200 to 800) and the number of hidden units of LSTM (200 to 1000). We also compared it with three representative classifiers, including the Support Vector Machine (SVM), Random Forest (RF) and Multilayer Perceptron (MLP). All classifiers used the same features best interpret comparisons across methods.

The SVM used radial basis function (RBF) kernel, and the kernel coefficient γ equals to 0.025. We set C equals to 0.5 to regularize the estimation in order to avoid noisy features. Shrinking heuristic is also applied. The RF used 100 estimators, and the performance of a split was estimated as

the mean square error. The number of features to consider when looking for best split was equal to the square root of number of features. The nodes of RF were expanded until the "leaves" are pure or until the "leaves" contain less than 2 samples. Both SVM and RF avoid class imbalances by setting class weight. The MLP in this comparison used 2 layers rectifying neuron followed by softmax output layer, and the random dropout was applied during supervised training. It is the same technique with the feature processing layer of the Mixed Neural Network. All hyper-parameters are fine-tuned to achieve it's best performance. Oversampling was used to avoid class imbalance problem when train the MLP.

We defined a rule for SVM, RF and MLP: If the sequence length (SL) is 1, we use only the features of current EEG epoch to train the classifier. If sequence length is 2, it means we train the classifier by using the features from current EEG epoch and previous 1 EEG epoch, and so on. In LSTM, sequence length is the number of example we are going to consider for each output.

The classification performance was evaluated by widely-used indexes: macro F1-score (MF1) and overall accuracy (ACC). While the MF1 reflects the mean of F1-score over all classes, the ACC reflects the accuracy across all EEG epochs from cross-validation. In addition, the performances of each individual stage were evaluated by using the recall (RE), precision (PR) and F1-score (F1).

In this experiment, the training and validation data are from different recordings in order to limit overfitting and data dependence. K-fold cross-validation was adopted, K was set to 32 for the 62 recordings, which means 2 recordings was used as a validation set and the other 60 recordings were used as a training set for each validation. To speed up the evaluation, Graphical Processing Units (GPU) acceleration was used to training the network. Training the networks for sequence length equal to 5 over cross validation takes about 2 days by using NVIDIA 630 GPU on a single machine. The code was implemented by Theano [28], [29].

III. EXPERIMENTAL RESULTS

TABLE IV
COMPARISONS OF DIFFERENT ALGORITHMS USING F4-EOG (LEFT)

SL	1	2	3	4	5
SVM					
MF1	73.43	75.01	74.71	74.34	73.92
ACC	78.01	79.70	79.53	79.20	78.87
RF					
MF1	69.95	72.07	72.44	71.70	71.32
ACC	80.68	81.53	81.67	81.30	81.18
MLP					
MF1	74.11	76.71	76.80	77.23	76.71
ACC	78.17	80.47	80.81	81.43	81.41
MNN					
MF1	73.71	78.49	79.76	80.35	80.50
ACC	82.67	84.60	85.28	85.67	85.92

Table IV shows the macro F1-score (MF1) and overall accuracy (ACC) of different classifiers from cross-validation under different sequence length, while the boldface numbers indicated the best performance of a classifier.

We found that the performance of control group (SVM, RF and MLP) shows slight improvement when using the features from previous EEG epoch(s) compared with using only the features from current EEG epoch (sequence length=1). However, there was no continual improvement found and the results even became worse as the sequence length increased. For example, the performance of SVM became worse when the sequence length increased from 2 to 5. The reason is the control group can only transfer the classification problem as a complex formula and not as sequential model. In this experiment, SVM reached its best performance when using the features from current and previous EEG epoch. RF and MLP gave their best performance by using features from 3 and 4 nearest EEG epochs, respectively. Moreover, RF has better accuracy compare with SVM and MLP, but its macro F1-score is the worst.

By contrast, both the macro F1-score and overall accuracy of the Mixed Neural Network showed continual improvements as the sequence length increased. As the nearer EEG epochs have bigger impact on current sleep stage, the increasing velocity decreases as the sequence length increases. The result demonstrated that our network has ability to remember the stage information epoch by epoch. Even setting the sequence length to 1, its accuracy is still better than the control group. When its sequence length is set to 5, both overall accuracy and macro F1-score become significantly higher than other classifiers. Table V shows its confusion matrix from cross-validation, the left column is the actual class labeled by sleep expert, and the top row is the predicted class calculated by the classifier.

For more details, Table VI compared MNN with the control group across different sleep stages. This table lists the best performance of different classifiers.

The boldface numbers indicated the best situation across classifiers in control group, and then the bottom line list the improvement of MNN compare with the control group. It is clear not only that MNN has better overall accuracy and macro F1-score, but also that all F1-scores for individual sleep stages are better than those for the control group overall.

TABLE V
CONFUSION MATRIX FROM CROSS-VALIDATION USING MNN AND F4-EOG (LEFT) WHEN SEQUENCE LENGTH IS 5

ACC = 85.92% MF1 = 80.50%									
SL=5	W	N1	N2	N3	REM	RE	PR	F1	
W	5022	577	188	19	395	80.95	88.49	84.55	
N1	407	2468	989	4	965	51.07	62.75	56.31	
N2	130	630	27254	1021	763	91.46	90.02	90.73	
N3	13	0	1236	6399	5	83.61	85.94	84.76	
REM	103	258	609	0	9611	90.83	81.87	86.12	

Compared with existing studies, Table VII shows their macro F1-scores, overall accuracy and the F1-scores of dif-

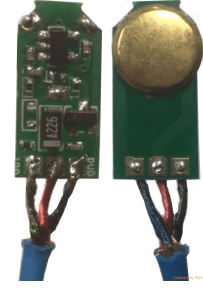


Fig. 3. Active ultra-high impedance electrode design(Left: circle side; Right: skin contact side)

ferent sleep stages. It shows that our macro F1-score, and F1-score of stage N1 and N2 are significantly higher than the existing studies. That is because LSTM can do better to deal to the continuation of N1 and N2. However, the F1-score of stage W is lower than most of existing studies. It is caused by poor detection of alpha rhythm from frontal lobe, but it still better than one study using EEG from central lobe.

In conclusion, the proposed Mixed Neural Network and the corresponding training method works well for sleep stages classification problem compared with SVM, RF and MLP. Moreover, the proposed method only uses EEG signal from a two paired electrodes placed in hairless positions. This ensures that they can be worn comfortably.

IV. DISCUSSION

We plan to apply the proposed algorithm with data from a wearable EEG device to achieve low-cost home-care sleep monitoring. The main design factors we have considered are: electrode position, comfort and desirability of a dry electrode contact. However, the trade-off between electrode position and classification performance needs to be considered, e.g., the greater the distance between the electrode and the occipital lobe, the poorer the performance of classifying stage W.

Dry electrodes have developed considerably over the last 10 years. Currently, there are 3 major categories of dry electrode: the ultra-high impedance electrode, the spiked electrode and the electro-optic electrode [27]. The outermost layer of the epidermis is called skin stratum corneum, consisting of dead cells, has a high resistance around $10^7\Omega$ that limits surface detection of deeper potential changes. In usual practice, a "wet" electrode uses an electrolytic gel to reduce the resistance of stratum corneum in conjunction with an amplifier having an input impedance of $10^8 - 10^{11}\Omega$. As an alternative, dry electrode, the ultra-high impedance electrode is the most mature technology. This design includes a built-in buffer amplifier with input impedance greater than or equal to 10^{12} which can detect potential change under deep to the stratum corneum without any conductive gel. Additionally, the direct metal-to-skin contact enables longer life. The major disadvantage of this type of electrode is that it requires an extra electrical circuit.

TABLE VIII
CONFUSION MATRIX FROM CROSS-VALIDATION USING MNN AND
Fp2-EOG (LEFT) WHEN SEQUENCE LENGTH IS 5

ACC = 83.35% MF1 = 76.97%

SL=5	W	N1	N2	N3	REM	RE	PR	F1
W	4604	795	294	32	479	74.21	86.04	79.69
N1	405	2208	1292	9	919	45.69	57.08	50.75
N2	208	605	27199	897	889	91.28	86.65	88.91
N3	24	1	1689	5936	3	77.56	86.22	81.66
REM	110	259	914	11	9287	87.77	80.22	83.83

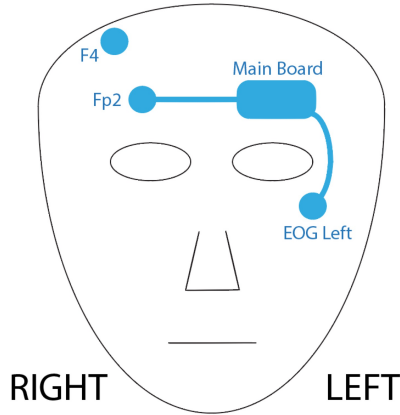


Fig. 4. Proposed home-care sleep monitoring configuration

In order to achieve real home-care sleep monitoring, an active ultra-high impedance electrode was designed as Fig. 3 shows. With the flat surface, this electrode is able to capture EEG well on the hairless skin. However, in terms of convenience, wearing the F4 channel near the hair line is imperfect. Other frontal EEG channels such as Fp2 and Fpz are easier to wear, but these channels have lesser information about stage W, N1, N2 and N3 compared with the F4 channel due to the longer distance to central lobe, as Table I describes. To evaluate these channels, Fp2-EOG left was evaluated by using the Mixed Neural Network and the same feature extraction algorithm with F4-EOG left. The result on Table VIII shows lower accuracy and macro F1-score compare with F4-EOG left. However, the result still better than other classifies in control group when they used EEG from F4-EOG left.

Fig. 4 illustrates the idea of home-care sleep monitoring system using Fp2-EOG left and dry electrode. The main board contains amplifiers, an analog to digital converter and wireless transmission module. The driven-right leg (DRL) can be placed on anywhere such as the back side of main board. With this structure, the device can be designed as a sleep mask, then movement during sleep would not lead to uncomfortable feeling and noisy signal.

APPENDIX A CONFUSION MATRICES OF EXISTING STUDIES

We need to point out these existing single-channel based studies used different dataset for evaluation, so it is not suitable to compare them directly by using accuracy. However, the recall, precision and F1-score can illustrate the reliability of

algorithms, especially for stage N1. The confusion matrices are borrowed from their papers.

TABLE I
EEG WAVES AND EVENTS DURING SLEEP

Event	Frequency/Duration	Best Location	Related Stage
Alpha rhythm [3]	8-13 Hz	Occipital lobe	W
Eye blinks	0.5-2 Hz	EOG channel	W
Reading eye movement	uncertain	EOG channel	W
Rapid eye movement [11]	0.5-2 Hz < 0.5 s	EOG channel	W, REM
Slow eye movement [12]	0.1-1 Hz > 0.5 s	EOG channel	N1
Low amplitude, mixed frequency activity [13]	4-7 Hz	Frontal and Central lobe	N1
Vertex shape waves	< 0.5 s	Central lobe	N1
K complex	1.6-4 Hz \geq 0.5 s	Frontal lobe	N2
Sleep spindle	11-16 Hz \geq 0.5 s	Central lobe	N2, N3
Major body movement	> 15 s	All channels	All stages
Slow wave activity	0.5-2 Hz > 75 μ V	Frontal lobe	N3
Low chin EMG tone	15-30 Hz	—	REM
Sawtooth waves	2-6 Hz	Central lobe	REM
Transient muscle activity	< 0.25 s	—	REM
Arousal	15-30 Hz	—	N1

TABLE III
EEG FEATURES EXTRACTION

Feature	Purpose	Related Stage
Maximum and minimum signal amplitude over the entire epoch	Capture the major body movement and peaks	All stages
Shannon entropy over the entire epoch	Capture the amplitude of vibration	All stages
Maximum and minimum signal amplitude using a sliding window	Capture the major body movement and peaks	All stages
0.06-0.1 Hz using a sliding window	Capture the slow eye movement	N1
0.1-0.3 Hz using a sliding window	Capture the slow eye movement	N1
0.3-0.5 Hz using a sliding window	Capture the slow eye movement	N1
0.5-1 Hz using a sliding window	Capture the slow eye movement	N1
0.5-2 Hz using a sliding window	Capture the eye blink, rapid eye movement and slow wave activity	W, REM, N3
1.6-4 Hz using a sliding window	Capture the K complex	N2
3-4.5 Hz using a sliding window	Capture the hypersynchrony for children	N1
4-7 Hz using a sliding window	Capture the low amplitude, mixed frequency activity and rhythmic anterior theta activity (5-7 Hz, for children)	N1
8-13 Hz using a sliding window	Capture the alpha rhythm	W
11-16 Hz using a sliding window	Capture the sleep spindle	N2, N3
15-30 Hz using a sliding window	Capture the low chin EMG tone	REM
For the frequency-band power capture using a sliding window, calculate it's maximum, minimum, mean, median and standard derivation	Capture the occasionally and continuous features	All stages
0.06-0.1 Hz over the entire epoch	Capture the slow eye movement	N1
0.1-0.3 Hz over the entire epoch	Capture the slow eye movement	N1
0.3-0.5 Hz over the entire epoch	Capture the slow eye movement	N1
0.5-1 Hz over the entire epoch	Capture the slow eye movement	N1

TABLE VI
COMPARISON BETWEEN OUR METHOD AND OTHER CLASSIFIERS ACROSS THE FIVE SCORING PERFORMANCE METRICS (PRECISION, RECALL, F1-SCORE, MACRO F1-SCORE, AND OVERALL ACCURACY) USING F4-EOG (LEFT)

Method	SL	MF1	ACC	W			N1			N2			N3			REM		
				RE	PR	F1	RE	PR	F1	RE	PR	F1	RE	PR	F1	RE	PR	F1
SVM	2	75.01	79.70	84.14	73.79	78.63	59.76	41.14	48.73	78.78	94.81	86.06	91.52	75.03	82.46	80.20	78.20	79.19
RF	3	72.44	81.67	77.73	78.70	78.21	23.60	68.69	35.13	93.03	83.49	88.00	76.05	87.78	81.50	82.65	76.35	79.38
MLP	4	77.23	81.43	83.30	82.62	82.95	58.47	49.11	53.38	78.89	94.77	86.10	95.09	69.70	80.44	88.11	78.91	83.26
MNN	5	80.50	85.92	80.95	88.49	84.55	51.07	62.75	56.31	91.46	90.02	90.73	83.61	85.94	84.76	90.83	81.87	86.12
		+3.27	+4.49			+1.59			+2.93			+2.73			+2.30			+2.86

TABLE VII
COMPARISON BETWEEN OUR METHOD AND THE LITERATURE ACROSS THE THREE SCORING PERFORMANCE METRICS (F1-SCORE, MACRO-F1 SCORE,
AND OVERALL ACCURACY)

Study	Channel	MF1	ACC	F1				
				W	N1	N2	N3	REM
[4]	Fpz-Cz	73.73	78.94	71.58	47.04	84.60	84.03	81.40
[5]	Cz-Pz	74.74	82.57	91.45	47.62	82.59	74.21	77.81
[6]	C3-A2/Pz-Oz	68.11	83.60	93.62	15.29	78.25	71.45	81.96
[7]	Cz-Pz	72.36	82.94	85.95	20.86	84.78	84.28	85.95
MNN	F4-EOG Left	80.50	85.92	84.55	56.31	90.73	84.76	86.12
		+5.76	+2.32	-6.90	+8.69	+5.95	+0.48	+0.17

TABLE IX
COMPLEX MORLET WAVELETS FROM FPZ-CZ USING STACKED SPARSE
AUTOENCODERS [4]

ACC = 78.94% MF1 = 73.73%

	W	N1	N2	N3	REM	RE	PR	F1
W	2744	441	34	23	138	81.18	64.01	71.58
N1	471	1654	262	8	366	59.91	38.73	47.04
N2	621	1270	13696	1231	760	77.92	92.53	84.60
N3	143	7	469	4966	6	88.82	79.74	84.03
REM	308	899	340	0	6164	79.94	82.92	81.40

TABLE X
CWT AND RENYI'S ENTROPY FROM CZ-PZ USING RANDOM FOREST
CLASSIFIER [5]

ACC = 82.57% MF1 = 74.74%

	W	N1	N2	N3	REM	RE	PR	F1
W	2407	89	111	38	40	89.65	93.33	91.45
N1	56	185	52	8	48	53.01	43.22	47.62
N2	69	85	1897	174	131	80.52	84.76	82.59
N3	14	9	86	482	3	81.14	68.37	74.21
REM	33	60	92	3	719	79.27	76.41	77.81

TABLE XI
MULTISCALE ENTROPY AND AUTOREGRESSIVE MODELS FROM C3-A2
OR PZ-OZ USING LINEAR DISCRIMINANT ANALYSIS [6]

ACC = 83.60% MF1 = 68.11%

	W	N1	N2	N3	REM	RE	PR	F1
W	1849	87	59	4	11	91.99	95.31	93.62
N1	69	24	12	3	20	18.75	12.90	15.29
N2	15	45	669	165	59	70.20	88.38	78.25
N3	0	1	1	224	0	99.12	55.86	71.45
REM	7	29	16	5	334	85.42	78.77	81.96

TABLE XII
SPECTRAL / TEMPORAL FEATURE EXTRACTION FROM CZ-PZ USING
FUZZY CLASSIFICATION [7]

ACC = 82.94% MF1 = 72.36%

	W	N1	N2	N3	REM	RE	PR	F1
W	1609	136	134	20	52	82.47	89.74	85.95
N1	88	85	41	1	24	35.56	14.76	20.86
N2	37	250	4534	467	139	83.55	86.05	84.78
N3	0	0	369	2303	0	86.19	82.46	84.28
REM	59	105	191	2	1749	83.05	89.05	85.95

APPENDIX B

CONFUSION MATRICES FROM CROSS-VALIDATION OF DIFFERENT CLASSIFIERS USING SAME FEATURES

In order to make a fair comparison, these algorithms used same features as well as the proposed method on Table V, and same feature extraction algorithm as well as Table VIII.

Moreover, as SVM, RF and MLP have their best performance when sequence lengths are 2, 3 and 4 respectively as Table IV shows, only the confusion matrices with best performance are shown.

TABLE XIII
SVM USING F4-EOG (LEFT) WHEN SEQUENCE LENGTH IS 2

ACC = 79.70% MF1 = 75.01%

SL=2	W	N1	N2	N3	REM	RE	PR	F1
W	5369	574	73	17	348	84.14	73.79	78.63
N1	713	2891	430	8	796	59.76	41.14	48.73
N2	536	2266	23479	2302	1219	78.78	94.81	86.06
N3	132	2	512	7004	3	91.52	75.03	82.46
REM	526	1295	270	4	8486	80.20	78.20	79.19

TABLE XIV
RF USING F4-EOG (LEFT) WHEN SEQUENCE LENGTH IS 3

ACC = 81.67% MF1 = 72.44%

SL=3	W	N1	N2	N3	REM	RE	PR	F1
W	4914	202	606	19	581	77.73	78.70	78.21
N1	743	1141	1709	1	1241	23.60	68.69	35.13
N2	250	160	27724	790	878	93.03	83.49	88.00
N3	17	0	1808	5820	8	76.05	87.78	81.50
REM	320	158	1358	0	8745	82.65	76.35	79.38

TABLE XV
MLP USING F4-EOG (LEFT) WHEN SEQUENCE LENGTH IS 4

ACC = 81.43% MF1 = 77.23%

SL=4	W	N1	N2	N3	REM	RE	PR	F1
W	5218	550	88	30	378	83.30	82.62	82.95
N1	609	2826	533	12	853	58.47	49.11	53.38
N2	258	1658	23508	3117	1258	78.89	94.77	86.10
N3	12	4	357	7277	3	95.09	69.70	80.44
REM	218	717	319	4	9323	88.11	78.91	83.26

ACKNOWLEDGMENTS

The authors would like to thank Center for advanced research in sleep medicine, University of Montreal for providing the data, especially like to thank Christian O'reilly for her helpful answers. They gratefully acknowledges support from the Edmond J. Safra Foundation and Lily Safra and the Imperial College Healthcare Trust Biomedical Research Centre. They are also grateful to Pan Wang for her valuable comments and suggestions to design the sleep mask.

REFERENCES

- [1] Ohayon, M. M: Epidemiology of insomnia: What we know and what we still need to learn. Sleep Medicine Reviews, 6(2), 97-111, 2002.
- [2] A. Rechtschaffen, A. Kales: A Manual of Standardized Terminology, Techniques and Scoring System for Sleep Stages of Human Subjects, Public Health Service, U.S. Government Printing Office, Washington, DC, 1968.

[3] Iber, C., Ancoli-Israel, S., Chesson Jr., A. L., & Quan, S. F: The AASM Manual for the Scoring of Sleep and Associated Events: Rules Terminology and Technical Specifications 1st ed, 2007.

[4] Tsinalis, O., Matthews, P. M., & Guo, Y: Automatic Sleep Stage Scoring Using Time-Frequency Analysis and Stacked Sparse Autoencoders. *Annals of Biomedical Engineering*, 2015.

[5] Fraiwan, L., Lweesy, K., Khasawneh, N., Wenz, H., & Dickhaus, H: Automated sleep stage identification system based on time-frequency analysis of a single EEG channel and random forest classifier. *Computer Methods and Programs in Biomedicine*, 108(1), 10-19, 2012.

[6] Liang, S. F., Kuo, C. E., Hu, Y. H., Pan, Y. H., & Wang, Y. H: Automatic stage scoring of single-channel sleep EEG by using multiscale entropy and autoregressive models. *IEEE Transactions on Instrumentation and Measurement*, 61(6), 1649-1657, 2012.

[7] Berthomier, C., Drouot, X., Herman-Stoica, M., Berthomier, P., Prado, J., Bokar-Thire, D., d'Ortho, M. Automatic analysis of single-channel sleep EEG: validation in healthy individuals. *Sleep*, 30(11), 1587-1595, 2007.

[8] PhysioNet: The Sleep-EDF database [Expanded]. <http://www.physionet.org/physiobank/database/sleep-edfx/>. Accessed Jan 2015.

[9] O'Reilly, C., Gosselin, N., Carrier, J., & Nielsen, T. Montreal archive of sleep studies: An open-access resource for instrument benchmarking and exploratory research. *Journal of Sleep Research*, 23(6), 628-635, 2014.

[10] Chi, Y. M., Jung, T., & Cauwenberghs, G: Dry-contact and Non-contact Biopotential. *IEEE Reviews in Biomedical Engineering*, 3, 106-119, 2010.

[11] Yetton, B. D., Niknazar, M., Duggan, K. A., McDevitt, E. A., Whitehurst, L. N., Sattari, N., & Mednick, S. C: Automatic Detection of Rapid Eye Movements (REMs): A machine learning approach. *Journal of Neuroscience Methods*, 259, 72-82, 2015.

[12] Cona, F., Pizza, F., Provini, F., & Magosso, E: An improved algorithm for the automatic detection and characterization of slow eye movements. *Medical Engineering & Physics*, 36(7), 954-61, 2014.

[13] Bonnie Robertson & Buddy Marshall & Margaret-Ann Carno: Polysomnography for the Sleep Technologist, 1st Edition Instrumentation, Monitoring, and Related Procedures, 134-135, 2013.

[14] Bandarabadi, M., Teixeira, C. A., Rasekhi, J., & Dourado, A. Epileptic seizure prediction using relative spectral power features. *Clinical Neurophysiology*, 126(2), 237-248, 2014.

[15] Cohen, M. X. *Analyzing Neural Time Series Data: Theory and Practice*. Cambridge, MA: MIT Press, 2014.

[16] Sabeti, M., Katebi, S., & Boostani, R. Entropy and complexity measures for EEG signal classification of schizophrenic and control participants. *Artificial Intelligence in Medicine*, 47(3), 263-274, 2009.

[17] Glorot, X., Bordes, A., & Bengio, Y: Deep Sparse Rectifier Neural Networks. *Aistats*, 15, 315-323, 2011.

[18] Lennie, P: The cost of cortical computation. *Current Biology*, 13, 493-497, 2003.

[19] Hinton, G., Srivastava, N., Krizhevsky, A., Sutskever, I., Salakhutdinov, R. R: Improving neural networks by preventing co-adaptation of feature detectors, 2012.

[20] Srivastava Nitish, Hinton, G., Krizhevsky, A., Sutskever, I., & Salakhutdinov, R. R: Dropout: A Simple Way to Prevent Neural Networks from Overfitting. *Journal of Machine Learning Research*, 5(Jun)(2), 1929-1958, 2014.

[21] Hochreiter, S., Hochreiter, S., Schmidhuber, J., & Schmidhuber, J: Long short-term memory. *Neural Computation*, 9(8), 1735-80, 1997.

[22] Bengio, Y: Learning Long-Term Dependencies with Gradient Descent is Difficult. *IEEE Transaction on Neural Networks*, 5, 1994.

[23] Gers, F. a, Schraudolph, N. N., & Schmidhuber, J: Learning Precise Timing with LSTM Recurrent Networks. *Journal of Machine Learning Research*, 3(1), 115-143, 2002.

[24] Greff, K., Srivastava, R. K., Koutník, J., Steunebrink, B. R., & Schmidhuber, J. LSTM: A Search Space Odyssey. *Conference on Neural Information Processing Systems (NIPS)*. 2015.

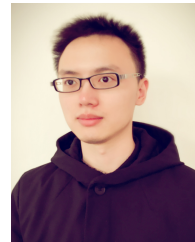
[25] Laon Bottou and Olivier Bousquet: The Tradeoffs of Large Scale Learning. *Advances in Neural Information Processing Systems (NIPS)*, 20:161aS168, 2007.

[26] Trans Cranial Technologies Ltd: 10 / 20 System Positioning Manual, 20. Retrieved from www.trans-cranial.com, 2012.

[27] Chi, Y. M., Jung, T., & Cauwenberghs, G: Dry-contact and Non-contact Biopotential. *IEEE Reviews in Biomedical Engineering*, 3, 106-119, 2010.

[28] F. Bastien, P. Lamblin, R. Pascanu, J. Bergstra, I. Goodfellow, A. Bergeron, N. Bouchard, D. Warde-Farley and Y. Bengio. Theano: new features and speed improvements. *Conference on Neural Information Processing Systems (NIPS)*, 2012.

[29] J. Bergstra, O. Breuleux, F. Bastien, P. Lamblin, R. Pascanu, G. Desjardins, J. Turian, D. Warde-Farley and Y. Bengio. Theano: A CPU and GPU Math Expression Compiler. *Proceedings of the Python for Scientific Computing Conference (SciPy)*, 2010.



Hao Dong received a first-class honours BEng degree in digital signal and image processing from Beijing Institute of Technology and University of Central Lancashire in 2011, and a Distinguish Master degree in Department of Computing (visual information processing group) from Imperial College London in 2012. He has held visiting position with Chinese Academy of Sciences. He also worked as a CTO at high-tech company in China.

He is now a Ph.D. candidate at Data Science Institute and Department of Computing, Imperial College London. His current research interests focus on deep learning, data acquisition and machine learning theory and applications in data driven research, especially in time series classification and automatic feature detection. He also concern about the field of advanced sensors. He is the recipient of Ph.D Scholarship and Outstanding Undergraduate Student Scholarship.



Akara Supratak received the B.Sc. degree in Information and Communication Technology (International Program) from the Faculty of Information and Communication Technology, Mahidol University, Thailand in 2010, and the M.Sc degree in Computing (Software Engineering) from Imperial College London, United Kingdom in 2013.

He is currently a Ph.D. candidate at Data Science Institute, Department of Computing, Imperial College London. His research interests includes biomedical engineering, software engineering and machine learning, especially with time series data.

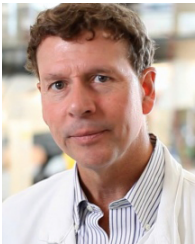


Wei Pan received the Ph.D. degree from Department of Bioengineering, Imperial College London in 2015. He received his Bachelor's degree in Automation from Harbin Institute of Technology in 2008 and Master's degree in Biomedical Engineering in 2011 from University of Science and Technology of China. He has held visiting positions with University of Luxembourg, Linkoping University and Huazhong University of Science and Technology. He also worked as a Quantitative Analyst at hedge fund in London.

He is now a Research Associate at Data Science Institute, Imperial College London. He is interested in machine learning theory and applications in data driven research especially in nonlinear time series modeling and prediction. He is the recipient of Dorothy Hodgkin Postgraduate Awards, Microsoft Research Ph.D. Scholarship and Chinese Government Award for Outstanding Students Abroad. He is an active reviewer for many international conferences and journals.



Chao Wu received his PhD degree from Zhejiang University, China. From 2011, he is now a Research Associate in the Discovery Science Group working on Elastic Sensor Network. His main research focus on data modelling and analysis, sensor network, social network (especially semantic social network), and mobile privacy.



Paul M. Matthews OBE, MD, DPhil, FRCP, FMed-Sci is Head of the new Division of Brain Sciences in the Department of Medicine of Imperial College, London. His research is noted for innovative translational applications of clinical imaging for the neurosciences. This has developed with exploitation of the powerful synergies between the physical and quantitative sciences and medicine.



Yike Guo received a first-class honours degree in Computing Science from Tsinghua University, China, in 1985 and received his Ph.D. in Computational Logic from Imperial College in 1993.

He is currently a Professor of Computing Science in the Department of Computing at Imperial College London. He is the founding Director of the Data Science Institute at Imperial College, as well as leading the Discovery Science Group in the department.